

Geochemistry of Mafic Rocks from the Birimian Basement of Doropo (Northeast of Côte d'Ivoire): Petrogenetic and Geodynamic Implications

Wilfried Digbeu^{1*}, Alain Nicaise Kouamelan¹, Asinne Tshibubudze², Ziandjêdé Hervé Siagne¹, Fossou Jean-Luc Hervé Kouadio¹

¹Laboratoire de Géologie, Ressources Minérales et Energétiques, Université Félix Houphouët-Boigny, Abidjan-Cocody, Côte d'Ivoire

²Council for Geosciences, Pretoria, South Africa

Email: *wilfrieddigbeu004@gmail.com

How to cite this paper: Digbeu, W., Kouamelan, A.N., Tshibubudze, A., Siagne, Z.H. and Kouadio, F.J.-L.H. (2022) Geochemistry of Mafic Rocks from the Birimian Basement of Doropo (Northeast of Côte d'Ivoire): Petrogenetic and Geodynamic Implications. *Open Journal of Geology*, 12, 504-520.

<https://doi.org/10.4236/ojg.2022.126024>

Received: May 19, 2022

Accepted: June 27, 2022

Published: June 30, 2022

Copyright © 2022 by author(s) and Scientific Research Publishing Inc. This work is licensed under the Creative Commons Attribution International License (CC BY 4.0).

<http://creativecommons.org/licenses/by/4.0/>



Open Access

Abstract

The northeastern region of Côte d'Ivoire is characterised by a granitic basement mainly composed of biotite granite rocks. According to mapping work in the Gbabédjou and Doropo areas, these Birimian granitoids are cut by gabbro dykes and amphibolite enclaves, which are the subject of this study. In order to better understand the role and the implication of mafic rocks in the Doropo basement emplacement, a multidisciplinary methodology integrating microscopic observations and geochemical analyses of major and trace elements was carried out on 4 samples considered representative of the outcrops studied. Green hornblende, clinopyroxene, and accessory sphene minerals are found in mafic mineral phases, according to petrographic research. Whole-rock analyses reveal that mafic samples with TiO_2 contents $< 2\%$ are poor in Ti and have both calc-alkaline and tholeiitic rock affinities. They are metaluminous with $A/CNK > 1.1$ ratios giving them an orogenic granite nature (I-type). Their REE patterns are moderately fractionated $(La/Sm)_N = 2.66 - 6.13$ and $(La/Yb)_N = 11.17 - 43.70$ with a very negative Eu anomaly $(Eu/Eu^* = 0.75 - 0.97)$. The multi-element diagrams are characterized by negative Nb-Ta anomalies and geotectonic studies have identified them as volcanic arc formations. All these characteristics allowed us to distinguish the Doropo mafic rocks as formations originating from the juvenile continental crust, emplaced under the Archean tectonics model with significant crustal contamination in the source. Magma driven by mantle diapir has been injected at the base of the continental crust and the heat induces the partial melting of the overlying

crust giving rise to mixed liquids. This magma now enriched in LILE was immediately drained to the upper crust to form the mafic rocks from the studied area.

Keywords

Doropo, Mafic Intrusive, Birimian, Crustal Contamination

1. Introduction

The Paleoproterozoic terrane of the Man-Leo Rise is described as greenstone belt assemblages associated with several generations of granitoid [1] [2] [3]. The study of the geodynamic setting of these Birimian-aged rocks has given rise to different opinions that can be summarized in two main tectonic assumptions. Indeed, some authors believe that the juvenile Birimian crust was produced in subduction-related environments [4] [5] [6] [7], while another school of thought suggests that it was generated by magmatism related to mantle plume [8] [9]. In order to provide arguments on the controversy related to the geodynamic evolution and growth of the Birimian continental crust, the mafic intrusives from the Gbabédjou and Doropo localities in northeastern Côte d'Ivoire were analyzed. This choice is based on the work of [10] who showed that to fully understand the evolution and overall tectonic setting of the Birimian rocks, particular attention should be paid to the mafic and ultramafic plutonic complexes and their associated intrusives. The objective of this paper is to characterize the gabbroic rocks of the Doropo region, using their major and trace element data. In other words, by integrating field work, petrography and whole-rock geochemistry, the study attempts to reveal the petrogenetic characteristics and implications of the mafic enclaves and dykes in the structuration of the Doropo Birimian basement.

2. Geological Setting

The Man-Leo Rise represents the Precambrian formations outcropping in the southern part of the West African Craton as two main domains (**Figure 1**). The Kenema-Man core consists mainly of Archean terrains, ranging in age from ~3.4 to 2.7 Ga, outcropping in western Côte d'Ivoire [11] [12], Guinea [13] [14], Sierra Leone and Liberia. In Côte d'Ivoire, this core is characterized by geological formations of the high degree of metamorphism such as grey granulite gneiss, charnockites, ultramafic rocks and granites [12] [15] [16]. Separated from the Archean Kénéma-Man domain by the Sassandra fault, the Baoulé-Mossi domain refers to the "Birimian" formations that occupy the eastern part of the rise. These terrains are consisting of belts of metavolcanic and metasedimentary rocks intruded by different generations of granitoids [17]-[22]. Whole rock geochemistry revealed that these different belts contain two main volcanic families. A tholeiitic mafic volcanic series at the base that is overlain by intermediate

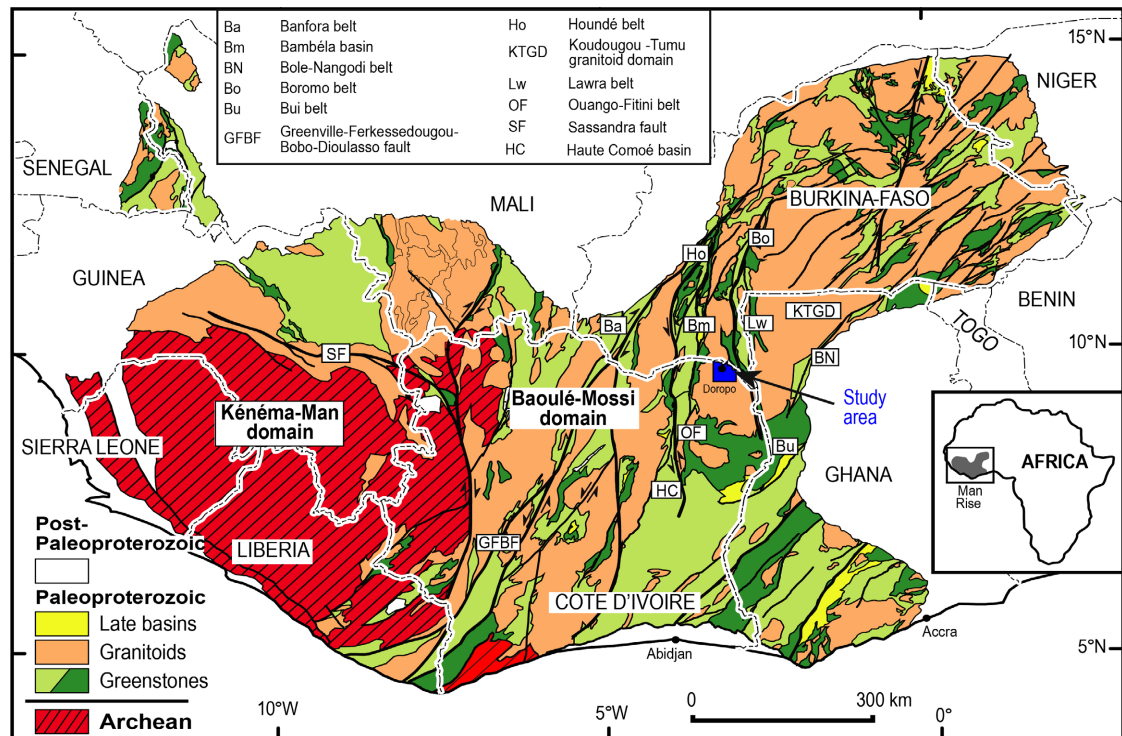


Figure 1. Simplified geological map of the Man-Leo Rise (modified after [29]).

acidic volcanic series of a calc-alkaline composition. Even with little scientific work the Doropo region, its geological setting can be apprehended, using the numerous studies completed in the adjacent localities [3] [23]-[28].

Structural studies [1] in the south of Burkina-Faso show that the Paleoproterozoic domain is composed of two greenstone belts oriented N-S, respectively, known as, from east to west: 1) Boromo Belt whose continuity in Ghana gives the Lawra Belt [3] and 2) Houndé Belt, which extends into Côte d'Ivoire as the Téhini Belt.

Work in north-eastern Ghana has shown that late Birimian basins filled with fine-grained sedimentary also occur in these belts. A sedimentary unit of the Tarkwaian type lies within and parallel to the Houndé belt, separated by shear zones on either side. These belts are separated by the Diébougou granitic domain in Burkina-Faso, whose continuity in Côte d'Ivoire corresponds to that of Doropo [23], which we call the Doropo Granitic Complex. This area was affected by significant surface weathering and scarcity of outcrops, which hinder cartographic surveying, mining exploration and therefore structural study. [30] has identified many lithological groups: Biotite granite, gneissic granite, granodiorite, gabbro, amphibolite, tonalite, rhyolite and dolerite (**Figure 2**). Recent works in the region, agree to distinguish four major groups of granitoids, corresponding to four magmatic episodes [1] [24]. The nature of these different granitoids (ME1 to ME4 at regional scale, according to WAXI project researchers) was constrained by radiometric and satellite geophysical data [3] [24] [25] [27].

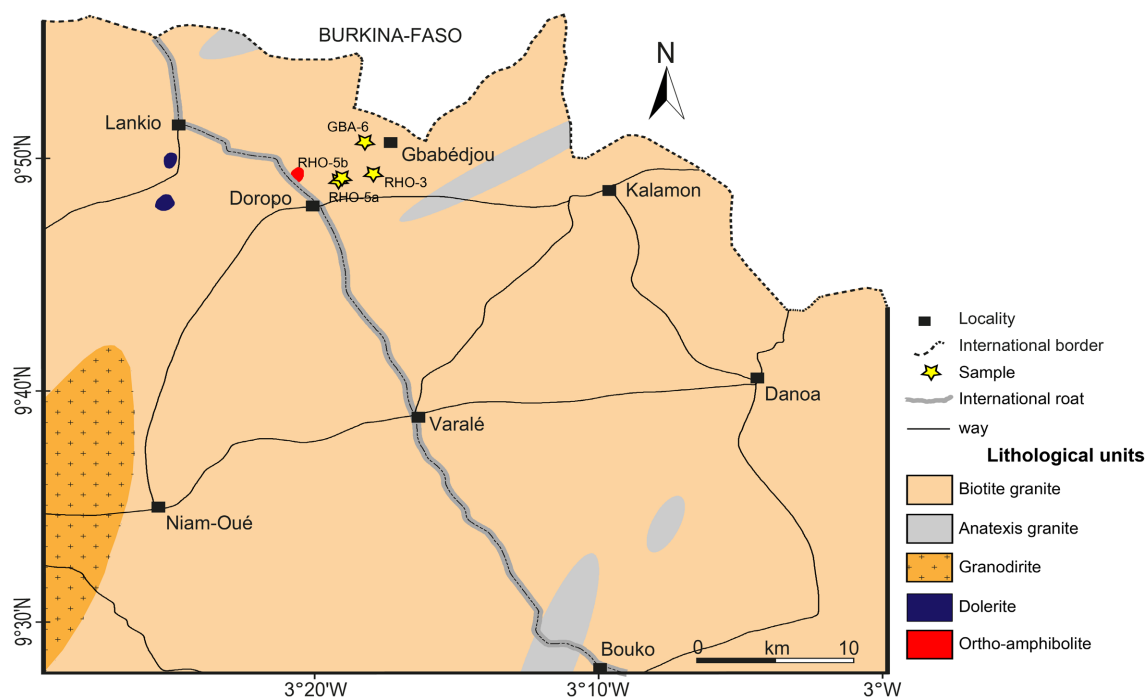


Figure 2. Geological map of Doropo area with location of analyzed samples.

3. Methodology

The study of the mafic intrusives of Doropo consisted of a sampling step followed by thin section preparation and geochemical analyses from 04 representative samples taken in the localities of Gbabédjou and Doropo (Figure 2).

The thin sections and their microscopic description were carried out at the Laboratory of Geology Mineral Resource and Energetic (LGRME) of University Félix Houphouët-Boigny of Abidjan-Cocody. Geochemical analyses on whole-rock were carried out by Bureau Veritas (Vancouver). In practice, major elements were analyzed by X-ray fluorescence using an XRF while REEs and trace elements were tested by inductively coupled plasma-mass spectrometry (ICP-MS) using an Agilent 7700× mass spectrometer. For major elements, approximately 0.5 g of the rock powder was mixed with ~3 - 6 g of $\text{Li}_2\text{B}_4\text{O}_7$, and ~3 - 4 drops of NH_4Br was added and the mixture fused in a furnace to form a glass disk. The disks were then analyzed using a current and voltage of 50 mA and ~50 kV, respectively. To quantify trace elements, about 100 mg of crushed whole-rock powder were dissolved in 2 ml HF and 1 ml HNO_3 in a closed Teflon bomb, which was heated on a hot plate at 140°C, then opened and subsequently evaporated to dryness to remove silica. After evaporation all samples were subjected to three steps of evaporation with decreasing HNO_3 quantities and at increasing temperatures up to 150°C to remove fluorides. Samples were then dissolved in 2% HNO_3 and diluted shortly before analysis to a final dilution factor of ca. 5000. Dilution factor were kept high to avoid detector saturation, and to minimize drift which was corrected for by addition of doping elements, namely In and Bi, at a concentration level of 1 ppb. The solutions were then analyzed using ICP-MS

analyses and analytical uncertainties were 1% - 3% relative to elements present in concentrations > 1 wt%, and about 10% relative to elements present in concentrations < 1 wt%. The instruments conditions are given in [31] and [32] while quality control of the analyses required the use of standard samples (DS11, GS311-1 and GS910-4) and the accuracy was better than 1%. Data processing and diagrams were done using GCD Kit 4.2 software [33].

4. Results

4.1. Petrographic Description

4.1.1. Gabbro

This lithological unit outcrops as a dyke through the biotite granite (**Figure 3(a)** and **Figure 3(b)**).

It is a massive rock, dark green and crossed by quartz and pegmatite veins at the contact zones with the granite. The thin sections analysis revealed a grained texture where green hornblende is present in very large quantities (**Figure 3(c)** and **Figure 3(d)**). This mineral appears under two habitus within the studied samples. The first habitus results from the partial or complete secondary alteration of clinopyroxene while the second, interstitial in size, appears igneous. The plagioclases are strongly altered, giving rise to sericite and sometimes epidote. Clinopyroxenes are less abundant and difficult to observe because of their alteration. In the contact zones with biotite granite, the samples show accumulation of biotite and quartz. Spene and some ferro-titanium minerals remain the primary accessory phases.

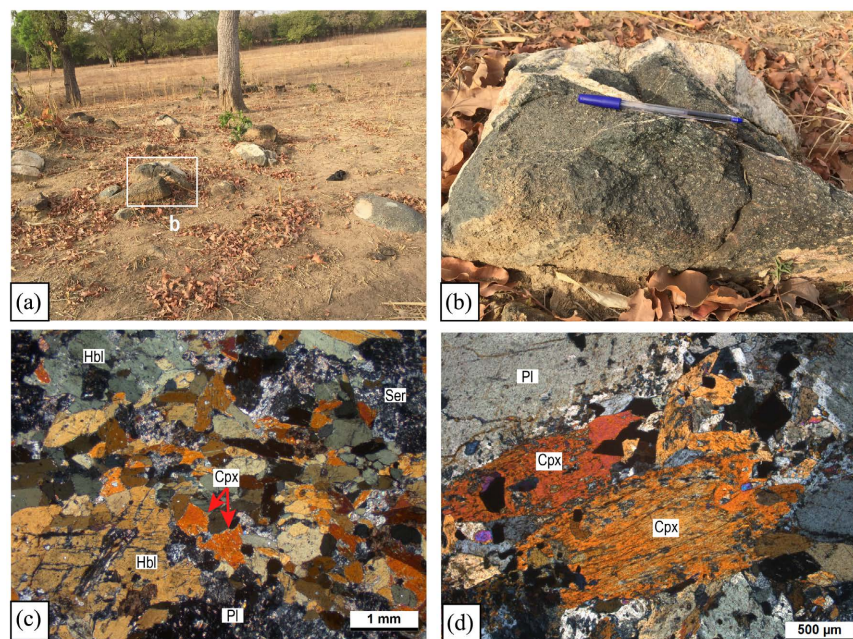


Figure 3. Macroscopic and microscopic aspects of Doropo gabbros. (a) Dyke of gabbro; (b) Gabbro sample in contact with biotite granite; (c) mineralogy of gabbro from Doropo; (d) altered clinopyroxene. (*Hbl*: hornblende, *Cpx*: clinopyroxene, *Pl*: plagioclase, *Ser*: sericite).

4.1.2. Amphibolite

Amphibolite generally outcrops as enclaves in biotite granite or granodiorite. This rock is also massive, green black and covered by a weak oxidation layer (**Figure 4(a)** and **Figure 4(b)**).

It is crossed by small rectilinear or wavy quartz veins, giving the appearance of a foliation. In terms of deformation, mineral lineation defined by hornblende and schistosity have been observed in the oval enclaves. Thin section study shows a medium-grained and nematoblastic texture (**Figure 4(c)** and **Figure 4(d)**). Sub-euhedral green hornblende forms the main mineral phase of the rock. Plagioclase exists throughout the rock in abundant quantities and is highly altered. Clinopyroxene is less abundant and similar in size to hornblende. Numerous small sphene crystals, sometimes included in the hornblende, constitute the primary accessory phase, while sericite and epidote are partly related to the destabilization of plagioclase.

4.2. Geochemistry of Doropo Mafic Intrusive

4.2.1. Classification

Table 1 gives the composition of major elements (wt%) and trace elements (ppm) of the mafic rocks of the Doropo area. For the samples analyzed, SiO₂ contents range from 48.00 to 50.80 wt% with the low values of loss on ignition (0.72% - 1.23%). Most of the samples are characterized by moderate to high Al₂O₃ (9.29 - 17.40 wt%), and CaO (9.88 - 14.0 wt%) contents, and variable Na₂O (2.07 - 3.65 wt%) and P₂O₅ contents (0.05 - 0.39 wt%) while TiO₂ concentrations

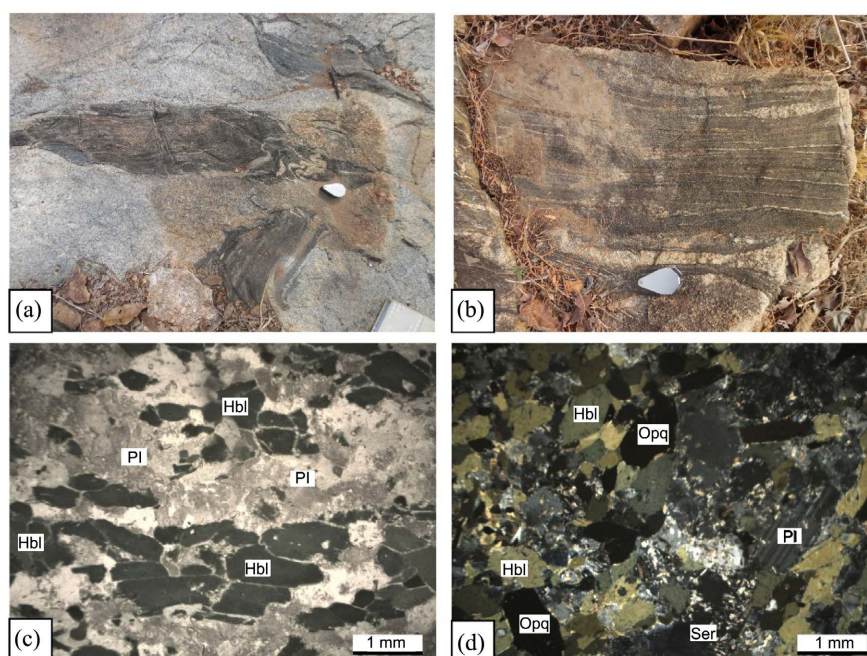


Figure 4. Petrographic aspects of the Gbabédjou amphibolite. (a) Enclaves of amphibolite in biotite granite; (b) Rectilinear and wavy quartz-veins giving a foliation appearance; (c) and (d) mineral composition of GBA-6 dominated by hornblende and plagioclase. (*Hbl*: hornblende, *Cpx*: clinopyroxene, *Pl*: plagioclase, *Ser*: sericite, *Opq*: opaque minerals).

Table 1. Major (%) and trace (ppm) elements composition of mafic rocks from Doropo.

| Rock type | Gabbro | | | Amphibolite |
|--------------------------------|--------|-------|-------|-------------|
| Sample number | RHO3 | RHO5a | RHO5b | GBA6 |
| Major elements (wt%) | | | | |
| SiO ₂ | 50.30 | 50.80 | 49.90 | 48.00 |
| Al ₂ O ₃ | 17.40 | 9.29 | 13.70 | 15.10 |
| Fe ₂ O ₃ | 8.70 | 9.47 | 8.19 | 13.30 |
| MnO | 0.13 | 0.17 | 0.15 | 0.20 |
| MgO | 6.54 | 11.10 | 9.40 | 6.14 |
| CaO | 9.88 | 13.90 | 14.00 | 10.30 |
| Na ₂ O | 3.65 | 2.07 | 2.28 | 3.52 |
| K ₂ O | 1.05 | 0.47 | 0.45 | 0.89 |
| TiO ₂ | 0.68 | 0.97 | 0.54 | 1.26 |
| P ₂ O ₅ | 0.05 | 0.39 | 0.10 | 0.11 |
| LOI | 1.23 | 0.99 | 1.17 | 0.72 |
| Total | 99.61 | 99.62 | 99.88 | 99.54 |
| Mg# | 0.46 | 0.57 | 0.56 | 0.33 |
| Trace elements (ppm) | | | | |
| Ba | 278 | 412 | 103 | 452 |
| Co | 8.3 | 7 | 44.7 | 6.8 |
| Cu | 25.4 | 25.9 | 75.3 | 41.4 |
| Ga | 22.6 | 19.8 | 10 | 18.1 |
| Hf | 4.1 | 5 | 1.9 | 6.7 |
| Nb | 6 | 6.7 | 3.8 | 17.8 |
| Ni | 7.9 | 5.4 | 20.4 | 5 |
| Pb | 1.8 | 1.4 | 1 | 2.6 |
| Rb | 61.6 | 69.2 | 17.5 | 70.5 |
| Sr | 469.6 | 466.8 | 277.2 | 413.1 |
| Ta | 0.5 | 0.6 | 0.2 | 2 |
| Th | 2.4 | 3.5 | 0.9 | 9.3 |
| U | 1.2 | 0.8 | 0.7 | 2.8 |
| V | 53 | 37 | 208 | 43 |
| Y | 19.8 | 7.5 | 27.9 | 21.6 |
| Zn | 63 | 83 | 19 | 77 |
| Zr | 180.3 | 210.6 | 72.7 | 270.2 |

Continued

| | | | | |
|--------------|--------|--------|--------|--------|
| La | 33.6 | 35 | 35.3 | 53.5 |
| Ce | 44.4 | 64.8 | 52.9 | 97.3 |
| Pr | 7.27 | 6.89 | 10.03 | 10.48 |
| Nd | 28.7 | 24 | 42.2 | 38.7 |
| Sm | 5.49 | 3.59 | 8.35 | 6.27 |
| Eu | 1.55 | 0.98 | 2.04 | 1.42 |
| Gd | 5.47 | 2.68 | 7.84 | 5.4 |
| Tb | 0.71 | 0.36 | 1.03 | 0.74 |
| Dy | 3.68 | 1.67 | 5.51 | 3.95 |
| Ho | 0.65 | 0.26 | 0.98 | 0.69 |
| Er | 1.69 | 0.72 | 2.45 | 1.89 |
| Tm | 0.2 | 0.08 | 0.31 | 0.25 |
| Yb | 1.16 | 0.54 | 2.13 | 1.5 |
| Lu | 0.19 | 0.08 | 0.3 | 0.22 |
| Σ REE | 134.76 | 141.65 | 171.37 | 222.31 |

remain below 2%. On Mg# [*i.e.* ratio of MgO/(MgO + FeOt)] values, all Doropo mafic rocks range from 0.33 to 0.57. The TAS diagram applied to the mafic rocks of the study area, allows to identify them as gabbros (**Figure 5(a)**). However, the amphibolite is alkaline and the gabbros correspond to sub-alkaline rocks according to the subdivision of [34]. In the FeOt/MgO vs SiO₂ diagram of [35], two evolutionary trends are highlighted by the studied samples (**Figure 5(b)**). The gabbros follow a calc-alkaline evolution while the amphibolite indicates a tholeiitic affinity. The A/NK vs. A/CNK diagram of [36] characterized the Doropo mafic intrusives as “metaluminous” rocks (**Figure 6**). Following this classification, no peraluminous or peralkaline mafic rocks were identified in the study area.

4.2.2. Geodynamic Context

The TiO₂-10 * MnO-10 * P₂O₅ ternary diagram of [37] shows that the mafic rocks of Doropo have the character of Island-type environment (**Figure 7**). Samples GBA-6, RHO-3 and RHO-5b are thought to be arc tholeiites while the RHO-5a gabbro is thought to be a calc-alkaline basalt.

4.2.3. Trace Elements Distribution

The gabbros have Rare Earth Elements contents (Σ REE) between 135 and 171 ppm and are characterized by slightly parallel patterns. Amphibolite GBA-6 with high concentrations of La and Ce has Σ REE = 222 ppm and its REE pattern remains similar to that of the gabbros (**Figure 8**). In general, the gabbros are highly fractionated, LREE-enriched [(La/Sm)_N = 2.66 - 6.13] and moderately

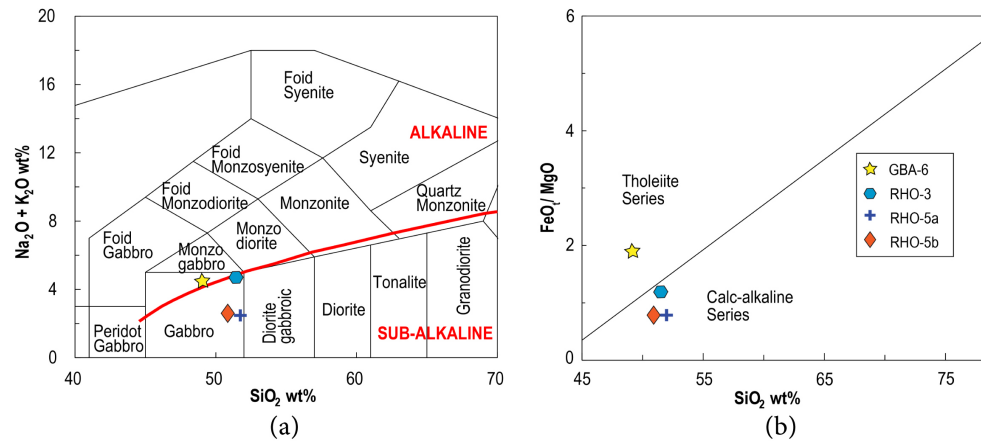


Figure 5. Nomenclature and magmatic series of the mafic rocks of Doropo. (a) TAS diagram applied to the analyzed samples, (b) FeO_t/MgO vs SiO₂ diagram.

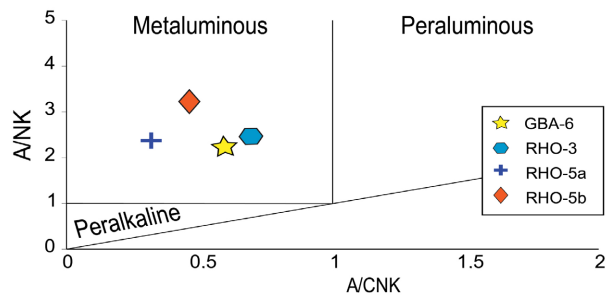


Figure 6. A/NK vs A/CNK diagram showing the geological evolution of the mafic rocks from Doropo area.

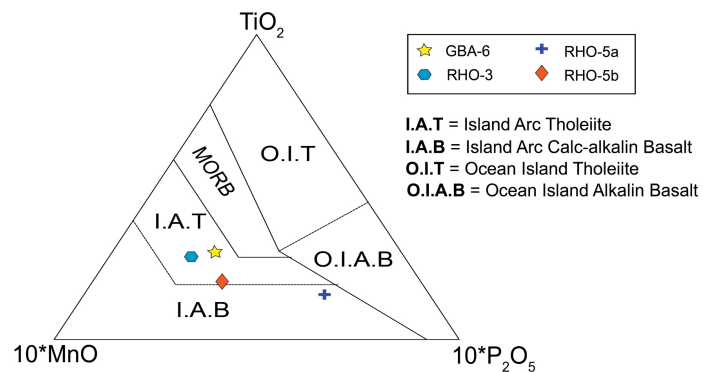


Figure 7. TiO₂-MnO * 10-P₂O₅ * 10 ternary diagrams showing island arc tectonic environment for studied samples.

HREE-depleted [(La/Yb)_N = 11.1; 7 - 43.70] with a negative Eu anomaly translated by Eu/Eu* = 0.75 - 0.97. For the gabbros, there is also a negative anomaly in Ce [with Ce/Ce* = 0.78 - 1.14]. From multi-element diagrams normalized to the early mantle [38], the Doropo mafic rocks are characterized by strong negative anomalies in Nb, Ta, P, Ti (Figure 9). Enrichments are reflected by U and La. These different geochemical signatures of the mafic rocks suggest significant crustal contamination.

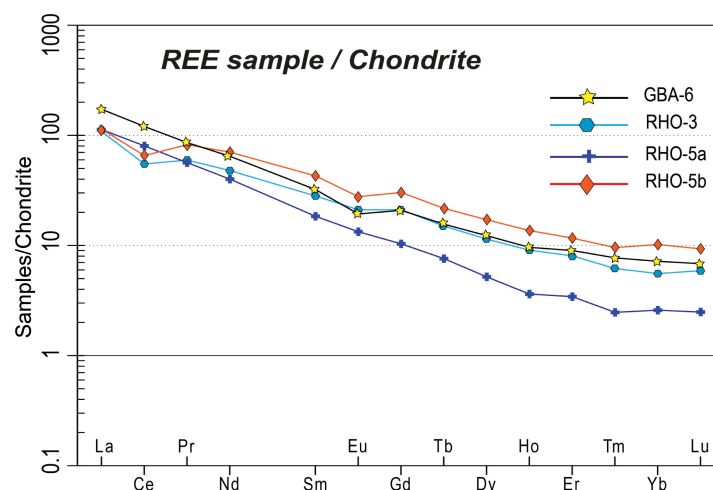


Figure 8. Chondrite-normalized REE patterns for Doropo mafic rocks. Chondrite normalising values are from [39].

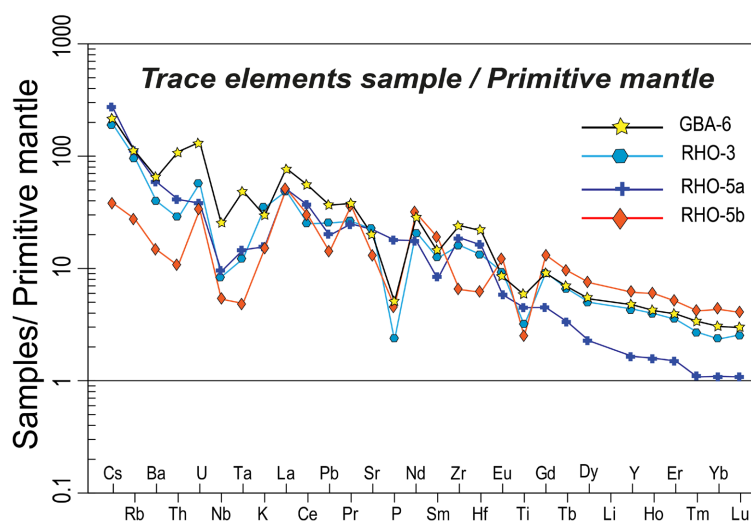


Figure 9. Primitive mantle normalised trace elements variation diagrams for Doropo mafic rocks. Normalisation factors from [38].

5. Discussion

Petrographic studies carried out in northeast of Côte d'Ivoire have highlighted the existence of mafic rocks in the granitic domain of the Doropo region [30]. These rocks, composed of gabbro dykes and amphibolite enclaves are characterized by a paragenesis mainly composed of green hornblende, plagioclase and clinopyroxene. This mineralogical composition is typical of mafic rocks described in the Birimian domain of the West African craton [10] [40] [41] [42]. The secondary paragenesis (epidote-sericite-hornblende) would be related to hydrothermal alteration or retrograde metamorphism of the Birimian massifs. On the basis of their SiO_2 and alkaline contents, most of these mafic rocks may be classified as gabbro, with calc-alkaline to moderately tholeiite affinity. Sample GBA-6 shows TiO_2 contents (1.26 wt%), which can be explained in terms of an

accumulation of ilmenite, titanite or hornblende. In fact, abnormal abundance of a TiO_2 -rich phase (hornblende specially) is petrographically observed in the gabbro samples from Doropo. Magmatic rocks derived from primary magma generally have high MgO, Mg#, and Ni contents (~ 15 wt%, >0.7 and >500 ppm, respectively). In contrast, samples from the study area show variable MgO (6.14 - 11.10 with an average of 8.3 wt%) and Ni < 50 ppm (Table 1). These data indicate that the Gbabédjou amphibolite and Doropo gabbros underwent a magmatic differentiation process before emplacement [43]. Regarding the magmatic source attributes of the studied rocks, their TiO_2 contents below 2%, similar to the mafic formations of the south-western Iberian massif [44], allows them to be interpreted as Ti-poor basalts. Similarly, the Zr/Ti ratio = 0.01 of the GBA-6 amphibolite and its Ni content = 14.8 ppm suggest an ortho-derivative magmatic origin according to [45]. The geochemical study also reveals that the Gbabédjou and Doropo samples have two possible lineages: tholeiitic and calc-alkaline. This is in agreement with the work of [46], [40] which in the Paleoproterozoic domain identify bimodal volcanism. The behaviour of immobile elements within the Doropo mafic rocks provides an argument that concerned samples do not represent a real composition of mantle-derived, probably reflecting that most of them must have undergone crustal contamination [44] [47]. In fact, mafic rocks are typically characterized by flat rare earth pattern with HFSE enrichment. However, the Doropo studied rocks are enriched in lithophile elements and slightly depleted in HFSE with negative anomalies in Nb-Ta especially reflecting crustal contamination. Also, with an average Nb/Yb ratio well above 2.95 characteristic value of E-MORBs according to [38] these rocks would be more favorable to the assumption of an oceanic crust or mantle source with crustal contamination [43]. In the La/Ba vs. La/Nb diagram (Figure 10), most samples fall outside the oceanic island basalts (OIB) indicating a lithospheric affinity or influence of crustal material during the formation of the Doropo basalts [43].

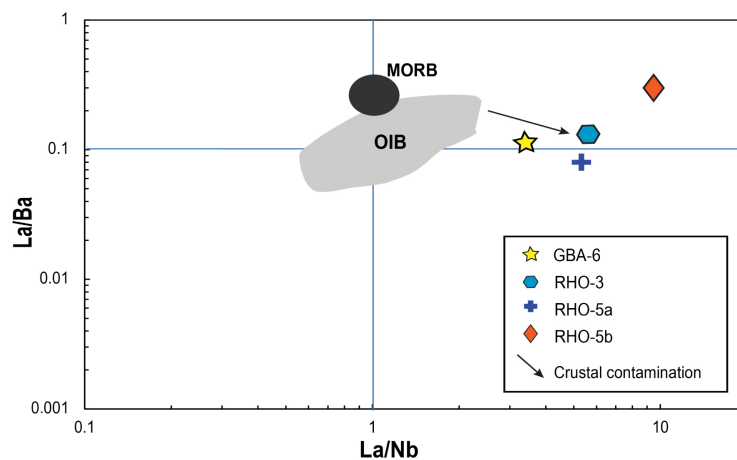


Figure 10. La/Ba vs La/Nb diagram showing the petrogenetic features of the Doropo mafic intrusive. Most of the samples plot in areas far from that of Ocean Island Basalts (OIB).

In other words, crustal contamination appears to have played an important role in the formation of these mafic intrusives. Based on trace element distribution and geotectonic evolution, we suggest that crustal contamination occurred in a subduction zone or during diapiric uplift in an Archean-type tectonic setting [11] [18] [48] [49] [50]. [23] showed that the rocks of this Birimian part of Côte d'Ivoire have TTG affinities, suggesting that their contamination would have occurred in an Archean-type geodynamic context. Indeed, the study area, characterized by a granite basement with fracture deformation giving rise to numerous dykes, is located between two large greenstone belts (Téhini and Lawra) corresponding to lithospheric structures [17] [51]. After the emplacement of the granitoid that constitute the Doropo Birimian basement, mantle-derived magma, driven by a diapir, is thought to have been injected at the base of the continental crust with an Archean TTG affinity [11]. The heat supplied by the basic liquid induces partial melting of the overlying crust giving rise to crustal anatectic liquids [52] [53]. These mixed incompletely with the basic component to give a contaminated magma enriched in lithophile elements, which was promptly drained to the upper crust to form the mafic "tholeiite" intrusives in the Doropo area. Also, this same magma, progressing slowly through the numerous dykes, has undergone both differentiation by fractional crystallization and significant mixing under the effect of flow in the rather narrow conduits. This would have allowed the formation of a second magma that was clearly more differentiated and more homogenized. This magma is thought to be the source of the "calc-alkaline" intrusive in the Doropo area. Similarly, referring to the work of [1] in the area of Gaoua, the hypothesis of crustal contamination during a horizontal tectonic regime particularly in the subduction modern-type zone would also seem probable for the Doropo rocks.

6. Conclusion

The mafic rocks of the Doropo area consist of gabbro and amphibolite outcropping as dykes and enclaves. These lithological units are characterised by mineralogy: hornblende, plagioclase, clinopyroxene, epidote, sericite, sphene and ferrotitanium minerals. Despite the existence of a secondary paragenesis due to the alteration of plagioclase and hornblende, the Gbabédjou amphibolite with Zr/Ti ratio = 0.01 and Ni = 14.8 ppm indicates a magmatic origin. Their Mg# range between 0.33 - 0.57 confirm that the studied sample is not cumulate but has low Ti-basaltic affinity. The distribution of trace elements shows that Doropo mafic intrusive are poorly enriched in HFSE and depleted in Nb, P and Ti, which are characteristic features of crustal contamination. Regarding geodynamic emplacement, the mafic rocks from Doropo correspond to crustal materials that evolved in an Archean-type geodynamic context. Magma driven by mantle diapir has been injected at the base of the continental crust with an Archean TTG affinity and the heat induces the partial melting of the overlying crust giving rise to mixed liquids. This magma enriched in lithophile elements was immediately drained to the upper crust to form the most of mafic rocks from the studied area.

Acknowledgements

This work is part of the projects financed by AMPELLA-CENTAMIN and supported by the Ministry of Higher Education and Scientific Research of Côte d'Ivoire (MESRS). The authors would like to thank Mrs. Fidèle KAKOU and Pier-rick COUDERC for their logistical support during field missions in the North-east of Côte d'Ivoire.

Conflicts of Interest

The authors declare no conflicts of interest regarding the publication of this paper.

References

- [1] Baratoux, L.L., Metelka, V., Naba, S., Jessell, M.W., Grégoire, M. and Ganne, J. (2011) Juvenile Paleoproterozoic Crust Evolution during the Eburnean Orogeny (~2.2-2.0 Ga), Western Burkina Faso. *Precambrian Research*, **191**, 18-45. <https://doi.org/10.1016/j.precamres.2011.08.010>
- [2] Perrouty, S., Aillères, L., Jessell, M.W., Baratoux, L., Bourassa, Y. and Crawford, B. (2012) Revised Eburnean Geodynamic Evolution of the Gold-Rich Southern Ashanti Belt, Ghana, with New Field and Geophysical Evidence of pre-Tarkwaian Deformations. *Precambrian Research*, **204-205**, 12-39. <https://doi.org/10.1016/j.precamres.2012.01.003>
- [3] Block, S., Ganne, J., Baratoux, L., Zeh, A., Parra, L.A., Jessell, M., Allères, L. and Siebenaller, L. (2016) Lower Crust Exhumation during Paleoproterozoic (Eburnean) Orogeny, NW Ghana, West African Craton: Interplay of Coeval Contractional Deformation and Extensional Gravitational Collapse. *Precambrian Research*, **274**, 82-109. <https://doi.org/10.1016/j.precamres.2015.10.014>
- [4] Mortimer, J. (1992) Lithostratigraphy of the Early Proterozoic Toumodi Volcanic Group in Central Côte d'Ivoire: Implications for Birrimian Stratigraphic Models. *Journal of African Earth Sciences (and the Middle East)*, **14**, 81-91. [https://doi.org/10.1016/0899-5362\(92\)90057-J](https://doi.org/10.1016/0899-5362(92)90057-J)
- [5] Sylvester, P.J. and Attoh, K. (1992) Lithostratigraphy and Composition of 2.1 Ga Greenstone Belts of the West African Craton and Their Bearing on Crustal Evolution and the Archean-Proterozoic Boundary. *The Journal of Geology*, **100**, 377-393. <https://doi.org/10.1086/629593>
- [6] Asiedu, D.K., Dampare, S.B., Sakyi, P.A., Banoeng-Yakubo, B., Osae, S., Nyarko, B.J.B. and Manu, J. (2004) Geochemistry of Paleoproterozoic Metasedimentary Rocks from the Birim Diamondiferous Field, Southern Ghana: Implications for Provenance and Crustal Evolution at the Archean-Proterozoic Boundary. *Geochemical Journal*, **38**, 215-228. <https://doi.org/10.2343/geochemj.38.215>
- [7] Dampare, S.B., Shibata, T., Asiedu, D.K., Osae, S. and Banoeng-Yakubo, B. (2008) Geochemistry of Paleoproterozoic Metavolcanic Rocks from the Southern Ashanti Volcanic Belt, Ghana: Petrogenetic and Tectonic Setting Implications. *Precambrian Research*, **162**, 403-423. <https://doi.org/10.1016/j.precamres.2007.10.001>
- [8] Abouchami, W., Boher, M., Michard, A. and Albarede, F. (1990) A Major 2.1 Ga Event of Mafic Magmatism in West Africa: An Early Stage of Crustal Accretion. *Journal of Geophysical Research: Solid Earth*, **95**, 17605-17629. <https://doi.org/10.1029/JB095iB11p17605>

- [9] Boher, M., Abouchami, W., Michard, A., Albarede, F. and Arndt, N.T. (1992) Crustal Growth in West Africa at 2.1 Ga. *Journal of Geophysical Research: Solid Earth*, **97**, 345-369. <https://doi.org/10.1029/91JB01640>
- [10] Abitty, E.K., Dampare, S.B., Nude, P.M. and Asiedu, D.K. (2016) Geochemistry and Petrogenesis of the K-Rich 'Bongo-Type' Granitoids in the Paleoproterozoic Bole-Nangodi Greenstone Belt of Ghana. *Journal of African Earth Sciences*, **122**, 47-62. <https://doi.org/10.1016/j.jafrearsci.2015.08.011>
- [11] Kouamelan, A.N., Delor, C. and Peucat, J.-J. (1997) Geochronological Evidence for Reworking of Archean Terrains during the Early Proterozoic (2.1 Ga) in the Western Cote D'Ivoire (Man Rise-West African Craton). *Precambrian Research*, **86**, 177-199. [https://doi.org/10.1016/S0301-9268\(97\)00043-0](https://doi.org/10.1016/S0301-9268(97)00043-0)
- [12] Koffi, G.R.-S., Kouamelan, A.N., Allialy, M.E., Coulibaly, Y. and Peucat, J.-J. (2020) Re-Evaluation of Leonian and Liberian Events in the Geodynamical Evolution of the Man-Leo Shield (West African Craton). *Precambrian Research*, **338**, Article ID: 105582. <https://doi.org/10.1016/j.precamres.2019.105582>
- [13] Thiéblemont, D., Goujou, J.C., Egal, E., Cocherie, A., Delor, C., Lafon, J.M. and Fanning, C.M. (2004) Archean Evolution of the Leo Rise and Its Eburnean Reworking. *Journal of African Earth Sciences*, **39**, 97-104. <https://doi.org/10.1016/j.jafrearsci.2004.07.059>
- [14] Eglinger, A., Thebaud, N., Zeh, A., Davis, J., Miller, J., Parra, L.A., Loucks, R., McCuaig, C. and Belousova, E. (2017) New Insights into the Crustal Growth of the Paleoproterozoic Margin of the Archean Kéména-Man Domain, West African Craton (Guinea): Implications for Gold Mineral System. *Precambrian Research*, **292**, 258-289. <https://doi.org/10.1016/j.precamres.2016.11.012>
- [15] Kouamelan, A.N., Djro, S.C., Allialy, M.E., Paquette, J.-L. and Peucat, J.-J. (2015) The Oldest Rock of Ivory Coast. *Journal of African Earth Sciences*, **103**, 65-70. <https://doi.org/10.1016/j.jafrearsci.2014.12.004>
- [16] Guedji, F., Picard, C., Coulibaly, Y., Audet, M.A., Auge, T., Goncalves, P. and Ouattara, N. (2014) The Samapleu Maficultramafic Intrusion and Its Ni-Cu-PGE Mineralization: An Eburnean (2.09 Ga) Feeder Dyke to the Yacouba Layered Complex (Man Archean Craton, Western Ivory Coast). *Bulletin de la Société Géologique de France*, **185**, 393-411. <https://doi.org/10.2113/gssgfbull.185.6.393>
- [17] Hirdes, W., Davis, D.W., Lüdtke, G. and Konan, G. (1996) Two Generations of Birimian (Paleo-Proterozoic) Volcanic Belts in Northeastern Côte d'Ivoire (West Africa): Consequences for the "Birimian Controversy". *Precambrian Research*, **80**, 173-191. [https://doi.org/10.1016/S0301-9268\(96\)00011-3](https://doi.org/10.1016/S0301-9268(96)00011-3)
- [18] Doumbia, S., Pouclet, A., Kouamelan, A., Peucat, J.J., Vidal, M. and Delor, C. (1998) Petrogenesis of Juvenile-Type Birimian (Paleoproterozoic) Granitoids in Central Côte-d'Ivoire, West Africa: Geochemistry and Geochronology. *Precambrian Research*, **87**, 33-63. [https://doi.org/10.1016/S0301-9268\(97\)00201-5](https://doi.org/10.1016/S0301-9268(97)00201-5)
- [19] Gasquet, D., Barbey, P., Adou, M. and Paquette, J.L. (2003) Structure, Sr-Nd Isotope Geochemistry and Zircon U-Pb Geochronology of the Granitoids of the Dabakala Area (Côte d'Ivoire): Evidence for a 2.3 Ga Crustal Growth Event in the Palaeoproterozoic of West Africa? *Precambrian Research*, **127**, 329-354. [https://doi.org/10.1016/S0301-9268\(03\)00209-2](https://doi.org/10.1016/S0301-9268(03)00209-2)
- [20] Naba, S., Lompo, M., Debat, P., Bouchez, J.L. and Béziat, D. (2004) Structure and Emplacement Model for Late-Orogenic Paleoproterozoic Granitoids: The Tenkogo-Yamba Elongate Pluton (Eastern Burkina Faso). *Journal of African Earth Sciences*, **38**, 41-57. <https://doi.org/10.1016/j.jafrearsci.2003.09.004>

- [21] Dioh, E., Béziat, D., Debat, P., Grégoire, M. and Ngom, P.M. (2006) Diversity of the Palaeoproterozoic Granitoids of the Kédougou Inlier (Eastern Sénégal): Petrographical and Geochemical Constraints. *Journal of African Earth Sciences*, **44**, 351-371. <https://doi.org/10.1016/j.jafrearsci.2005.11.024>
- [22] Ilboudo, H., Sawadogo, S., Kagambega, N. and Remmal, T. (2021) Petrology, Geochemistry, and Source of the Emplacement Model of the Paleoproterozoic Tiébélé Granite Pluton, Burkina Faso (West-Africa): Contribution to Mineral Exploration. *International Journal of Earth Sciences*, **110**, 1753-1781. <https://doi.org/10.1007/s00531-021-02039-3>
- [23] Vidal, M., Gumiaux, C., Cagnard, F., Pouclet, A., Ouattara, G. and Pichon, M. (2009) Evolution of a Paleoproterozoic “Weak Type” Orogeny in the West African Craton (Ivory Coast). *Tectonophysics*, **477**, 145-159. <https://doi.org/10.1016/j.tecto.2009.02.010>
- [24] Metelka, V., Baratoux, L., Naba, S. and Jessell, M.W. (2011) A Geophysically Constrained Litho-Structural Analysis of the Eburnean Greenstone Belts and Associated Granitoid Domains, Burkina Faso, West Africa. *Precambrian Research*, **190**, 48-69. <https://doi.org/10.1016/j.precamres.2011.08.002>
- [25] Baratoux, L., Metelka, V., Siebenaller, L., Naba, S., Naré, A., Ouyi, P., Jessell, M.W., Béziat, D., Salvi, S. and Franceschi, G. (2015) Tectonic Evolution of the Gaoua Region, Burkina Faso: Implications for Mineralization. *Journal of African Earth Sciences*, **112**, 419-439. <https://doi.org/10.1016/j.jafrearsci.2015.10.004>
- [26] Augustin, J. and Gaboury, D. (2015) Paleoproterozoic Plume-Related Basaltic Rocks in the Mana Gold District in Western Burkina Faso, West Africa: Implications for Exploration and the Source of Gold in Orogenic Deposits. *Journal of African Earth Sciences*, **129**, 17-30. <https://doi.org/10.1016/j.jafrearsci.2016.12.007>
- [27] Amponsah, P.O., Salvi, S., Béziat, D., Siebenaller, L., Baratoux, L. and Jessell, M.W. (2015) Geology and Geochemistry of the Shear-Hosted Julie Gold Deposit, NW Ghana. *Journal of African Earth Sciences*, **112**, 505-523. <https://doi.org/10.1016/j.jafrearsci.2015.06.013>
- [28] Grenholm, M., Jessell, M. and Thébaud, N. (2019) A Geodynamic Model for the Paleoproterozoic (ca. 2.27-1.96 Ga) Birimian Orogen of the Southern West African Craton—Insights into an Evolving Accretionary-Collisional Orogenic System. *Earth-Science Reviews*, **192**, 138-193. <https://doi.org/10.1016/j.earscirev.2019.02.006>
- [29] Milési, J.P., Feybesse, J.L., Pinna, P., Deschamps, Y., Kampunzu, H., Muhongo, S., Lescuyer, J.L., Le Golf, E., Delor, C., Billa, M., Ralay, F. and Henry, C. (2004) Geological Map of Africa 1:10,000,000, SIGAfrique Project. *20th Conference of African Geology, BRGM*, Orléans, June 2004, 2-7.
- [30] Siagné, Z.H., Aïfa, T., Kouamelan, A.N., Houssou, N.N. and Digbeu, W. (2021) Analyse Structurale De La Déformation Dans Les Granitoïdes Éburnéens De La Région De Doropo (Nord-Est De La Côte d’Ivoire). *European Scientific Journal*, **17**, 157-172. <https://doi.org/10.19044/esj.2021.v17n29p157>
- [31] Skursch, O., Tegner, C., Lesher, C.E. and Cawthorn, R.G. (2020) Two Expressions of the Transition from Mafic Cumulates to Granitoids in the Bushveld Complex, South Africa: Examples from the Western and Eastern Limbs. *Lithos*, **372-373**, Article ID: 105671. <https://doi.org/10.1016/j.lithos.2020.105671>
- [32] Eggins, S.M. (2003) Laser Ablation ICP-MS Analysis of Geological Materials Prepared as Lithium Borate Glasses. *Geostandard Newsletter*, **27**, 147-162. <https://doi.org/10.1111/j.1751-908X.2003.tb00642.x>
- [33] Janousek, V., Farrow, C.M. and Erban, V. (2006) Interpretation of Whole-Rock

- Geo-Chemical Data in Igneous Geochemistry: Introducing Geochemical Data Toolkit (GCDkit). *Journal of Petrology*, **47**, 1255-1259. <https://doi.org/10.1093/petrology/egl013>
- [34] Irvine, T.N. and Baragar, W.R.A. (1971) A Guide to the Chemical Classification of the Common Volcanic Rocks. *The Canadian Journal of Earth Sciences*, **8**, 523-548. <https://doi.org/10.1139/e71-055>
- [35] Miyashiro, A. (1974) Volcanic Rock Series in Island Arcs and Active Continental Margins. *American Journal of Science*, **274**, 321-355. <https://doi.org/10.2475/ajs.274.4.321>
- [36] Maniar, P.D. and Piccoli, P.M. (1989) Tectonic Discrimination of Granitoids. *GSA Bulletin*, **101**, 635-643. [https://doi.org/10.1130/0016-7606\(1989\)101<0635:TDOG>2.3.CO;2](https://doi.org/10.1130/0016-7606(1989)101<0635:TDOG>2.3.CO;2)
- [37] Mullen, E.D. (1983) MnO/TiO₂/P₂O₅: A Minor Element Discriminant for Basaltic Rocks of Oceanic Environments and Its Implications for Petrogenesis. *Earth and Planetary Science Letters*, **62**, 53-62. [https://doi.org/10.1016/0012-821X\(83\)90070-5](https://doi.org/10.1016/0012-821X(83)90070-5)
- [38] Sun, S.-S. and McDonough, W.F. (1989) Chemical and Isotopic Systematics of Oceanic Bas Basalts: Implications for Mantle Composition and Processes. *Geological Society, London, Special Publications*, **42**, 313-345. <https://doi.org/10.1144/GSL.SP.1989.042.01.19>
- [39] Boynton, W.V. (1984) Chapter 3. Cosmochemistry of the Rare Earth Elements: Meteorite Studies. In: Henderson, P., Ed., *Developments in Geochemistry*, Vol. 2, Elsevier, Amsterdam, 63-114. <https://doi.org/10.1016/B978-0-444-42148-7.50008-3>
- [40] Anum, S., Sakyi, P.A., Su, B., Nude, P.M., Nyame, F., Asiedu, D. and Kwayisi, D. (2015) Geochemistry and Geochronology of Granitoids in the Kibi-Asamankese Area of the Kibi-Winneba Volcanic Belt, Southern Ghana. *Journal of African Earth Sciences*, **102**, 166-179. <https://doi.org/10.1016/j.jafrearsci.2014.11.007>
- [41] Koffi, A.Y., Kouamelan, A.N., Djro, S.C., Kouadio, F.J.-L.H., Teha, K.R., Kouassi, B.R. and Koffi, G.R.S. (2018) Pétrographie et origine des métasédiments du domaine SASCA (SW de la Côte d'Ivoire). *International Journal of Innovation and Applied Studies*, **23**, 451-464.
- [42] Labou, I., Benoit, M., Baratoux, L., Grégoire, M., Ndiaye, M.P., Thebaud, N. and Debat, P. (2020) Petrological and Geochemical Study of Birimian Ultramafic Rocks within the West African Craton: Insights from Mako (Senegal) and Loraboué (Burkina Faso) Lher-Zolite/Harzburgite/Wehrlite Associations. *Journal of African Earth Sciences*, **162**, Article ID: 103677. <https://doi.org/10.1016/j.jafrearsci.2019.103677>
- [43] Wang, J., Wang, X., Liu, J., Liu, Z., Zhai, D. and Wang, Y. (2019) Geology, Geochemistry, and Geochronology of Gabbro from the Haoyaerhudong Gold Deposit, Northern Margin of the North China Craton. *Minerals*, **9**, Article No. 1. <https://doi.org/10.3390/min9010063>
- [44] Gómez-Pugnaire, M.T., Azor, A., Fernández-Soler, J.M. and López Sánchez-Vizcaíno, V. (2003) The Amphibolites from the Ossa-Morena/Central Iberian Variscan Suture (Southwestern Iberian Massif): Geochemistry and Tectonic Interpretation. *Lithos*, **68**, 23-42. [https://doi.org/10.1016/S0024-4937\(03\)00018-5](https://doi.org/10.1016/S0024-4937(03)00018-5)
- [45] Winchester, J.A. and Max, M.D. (1982) The Geochemistry and Origins of the Precambrian Rocks of the Rosslare Complex, SE Ireland. *Journal of the Geological Society*, **139**, 309-319. <https://doi.org/10.1144/gsjgs.139.3.0309>
- [46] Pouclet, A., Vidal, M., Delor, C., Simeon, Y. and Alric, G. (1996) Le volcanisme birimien du nord-est de la Côte d'Ivoire, mise en évidence de deux phases volcano-tectoniques distinctes dans l'évolution géodynamique du Paleoproterozoïque. *Bulletin de la Société*

- Géologique de France*, **167**, 529-541.
- [47] Saccani, E. (2015) A New Method of Discriminating Different Types of Post-Archean Ophiolitic Basalts and Their Tectonic Significance Using Th-Nb and Ce-Dy-Yb Systematics. *Geoscience Frontiers*, **6**, 481-501.
<https://doi.org/10.1016/j.gsf.2014.03.006>
- [48] Floyd, P.A. and Winchester, J.A. (1975) Magma Type and Tectonic Setting Discrimination Using Immobile Elements. *Earth and Planetary Science Letters*, **27**, 211-218.
[https://doi.org/10.1016/0012-821X\(75\)90031-X](https://doi.org/10.1016/0012-821X(75)90031-X)
- [49] Sajona, F.G., Maury, R.C., Bellon, H., Cotten, J. and Defant, M. (1996) High Field Strength Element Enrichment of Pliocene-Pleistocene Island Arc Basalts, Zamboanga Peninsula, Western Mindanao (Philippines). *Journal of Petrology*, **37**, 693-726.
<https://doi.org/10.1093/petrology/37.3.693>
- [50] Wane, O., Liégeois, J.-P., Thébaud, N., Miller, J., Metelka, V. and Jessell, M. (2018) The Onset of the Eburnean Collision with the Kenema-Man Craton Evidenced by Plutonic and Volcanosedimentary Rock Record of the Massigui Region, Southern Mali. *Precambrian Research*, **305**, 444-478.
<https://doi.org/10.1016/j.precamres.2017.11.008>
- [51] Lompo, M. (2010) Paleoproterozoic Structural Evolution of the Man-Leo Shield (West Africa). Key Structures for Vertical to Transcurrent Tectonics. *Journal of African Earth Sciences*, **58**, 19-36. <https://doi.org/10.1016/j.jafrearsci.2010.01.005>
- [52] Lompo, M. (2009) Geodynamic Evolution of the 2.25-2.0 Ga Palaeoproterozoic Magmatic Rocks in the Man-Leo Shield of the West African Craton. A Model of Subsidence of an Oceanic Plateau. *Geological Society, London, Special Publications*, **323**, 231-254. <https://doi.org/10.1144/SP323.11>
- [53] Smithies, R.H., Lu, Y., Johnson, T.E., Kirkland, C.L., Cassidy, K.F., Champion, D.C. and Poujol, M. (2019) No Evidence for High-Pressure Melting of Earth's Crust in the Archean. *Nature Communications*, **10**, Article No. 1.
<https://doi.org/10.1038/s41467-019-13547-x>